

Hierarchical forecasting for aggregated curves with an application to day-ahead electricity price auctions

Paul Ghelasi*, Florian Ziel†
University of Duisburg-Essen, Germany

May 26, 2023

Abstract

Aggregated curves are common structures in economics and finance, and the most prominent examples are supply and demand curves. In this study, we exploit the fact that all aggregated curves have an intrinsic hierarchical structure, and thus hierarchical reconciliation methods can be used to improve the forecast accuracy. We provide an in-depth theory on how aggregated curves can be constructed or deconstructed, and conclude that these methods are equivalent under weak assumptions. We consider multiple reconciliation methods for aggregated curves, including previously established bottom-up, top-down, and linear optimal reconciliation approaches. We also present a new benchmark reconciliation method called 'aggregated-down' with similar complexity to bottom-up and top-down approaches, but it tends to provide better accuracy in this setup. We conducted an empirical forecasting study on the German day-ahead power auction market by predicting the demand and supply curves, where their equilibrium determines the electricity price for the next day. Our results demonstrate that hierarchical reconciliation methods can be used to improve the forecasting accuracy of aggregated curves.

Keywords: Aggregation, coherent forecasts, reconciliation, hierarchical time series, forecast combinations.

*Corresponding author. Email addresses: paul.ghelasi@mail.com; paul.ghelasi@stud.uni-due.de

†Chair of Environmental Economics, esp. Economics of Renewable Energy. Email address: florian.ziel@uni-due.de

1 Introduction and motivation

Curves are frequently encountered structures in various scientific disciplines, and especially in economics and finance. Prominent examples are supply and demand curves [Marshall, 2009, Mankiw, 2014, Pindyck et al., 1995]. Other well-known examples are forwards and futures price curves [Hull, 2003], yield curves [Gürkaynak et al., 2007], Engel curves [Aitchison and Brown, 1954, Banks et al., 1997], Philips curve [Phillips, 1958], and various types of cost curves [Pindyck et al., 1995, Eiteman and Guthrie, 1952]. The accurate estimation of these curves is important because other measures such as equilibrium values can be derived from them, and modeling a curve as a whole has the benefit of preserving additional information such as its shape or slope, which could be very useful in deriving the strategies of market participants, equilibrium values, or probabilistic forecasts, rather than modeling the equilibrium prices directly [Ziel and Steinert, 2016].

It is important to note that we refer to curves as a single observation at a point in time, as is the case in functional data analysis (FDA) [Shang and Hyndman, 2017, Hyndman and Ullah, 2007, Shang and Hyndman, 2011]. In this study, we consider finite-dimensional representations of curves given by a finite grid of x -values and their corresponding y -values, often referred to as $f(x)$. Every curve with well-defined increments can be readily aggregated or disaggregated into marginal and cumulative values. For example, Figure 1 shows a simulated curve and its corresponding marginal values at each step. The cumulative values can be obtained from the marginal values by cumulatively summing them up, and the marginal values can be obtained from the cumulative values by discrete differentiation. Hence, from a computational point of view, a curve is simply a vector of aggregated values. This inherent structure of aggregated curves can be interpreted as a hierarchy, and thus hierarchical time series theory can be applied to potentially improve the forecasting accuracy [Hyndman and Athanasopoulos, 2018].

An hierarchical time series is a set of time series that naturally relate to each other, i.e. sum up or break down, according to a certain logic [Hyndman and Athanasopoulos, 2018, Wickramasuriya et al., 2019, Spiliotis et al., 2021]. This property is referred to as *coherency* and it is generally not given for individual forecasts. Approaches that allow independently forecasted time series at certain or all levels of the hierarchy to be made coherent are referred to as *reconciliation* methods.

Notable advances have been recently made in optimal reconciliation approaches as well

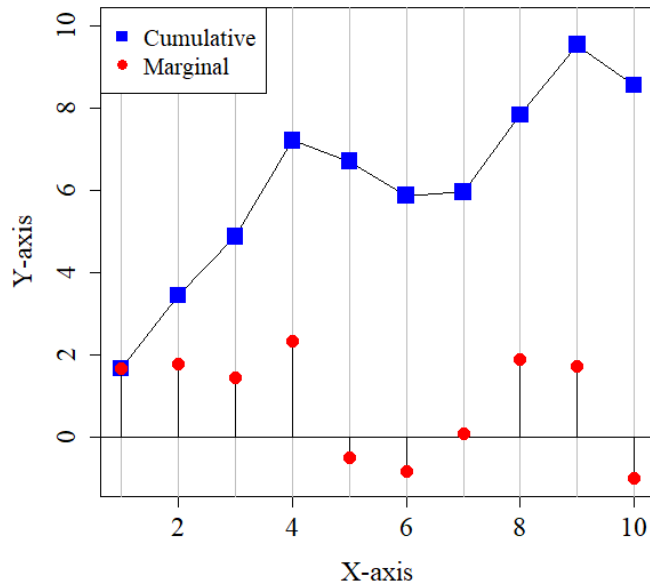


Figure 1: Example curve with marginal steps

as in improving classic approaches, such as top-down and bottom-up approaches, in terms of their forecasting accuracy Hyndman and Athanasopoulos [2018]. Most notable is the optimal *minimum trace* reconciling method Wickramasuriya et al. [2019]. Other methods have also been proposed, such as a *game-theoretically optimal* reconciliation approach [Van Erven and Cugliari, 2015], averaging approaches called *level conditional coherent* (LCC) and *combined conditional coherent* (CCC) point forecasts [Di Fonzo and Girolimetto, 2021, Hollyman et al., 2021] and machine-learning based reconciliation [Spiliotis et al., 2021], [Br eg ere and Huard, 2022], [Huard et al., 2020].

In this study, we introduce four novel features into the field of hierarchical forecasting. First, we exploit the fact that all aggregated curves have an implicit hierarchical structure and that reconciliation approaches can be used to potentially improve their forecast accuracy. To our knowledge, this is the first time that aggregated curves have been treated as hierarchical structures. We consider various methods of constructing and deconstruction the curves, including different representations of aggregated curves. Second, we introduce a new, simple reconciliation approach called *aggregated-down* with similar complexity to the top-down approach, which we recommend using as a benchmark method

alongside bottom-up and top-down approaches. Third, we study minimum trace optimal reconciliation approaches for aggregated curves in detail. In particular, we provide a result to show that under some assumptions, the reconciliation approach is independent of the representation of the curve. Finally, we applied all of these approaches in an empirical setting to forecast the supply and demand curves for day-ahead electricity price auctions. We conclude that forecast accuracy can be improved through hierarchical reconciliation.

To assess the effect of hierarchical reconciliation approaches on aggregated curves in an empirical setting we consider an application to the German day-ahead electricity markets. In this auction-based market, submitted bids are aggregated to form supply and demand curves [Narajewski and Ziel, 2022]. The intersection of the curves yields the day-ahead electricity price. Hence, the market mechanism itself fits our idea of aggregated curves, and thus the application of hierarchical forecasting is a natural extension.

Ziel and Steinert [2016, 2018], Haben et al. [2021a] forecast the day-ahead electricity price by forecasting the corresponding bids, aggregating them to form supply and demand curves, and computing the resulting intersection of these curves to yield the final price forecasts. This implicit application of the simple bottom-up reconciliation approach improved both point and probabilistic price forecasts. Recent related papers Kulakov [2020], Mestre et al. [2020], Soloviova and Vargiolu [2021] which forecast electricity supply and demand curves show similar findings.

The remainder of this paper is organized as follows. In Section 2, we introduce the notation for the inherent hierarchical structure of aggregated curves. We also describe different ways to construct and represent curves via aggregation and/or disaggregation. In Section 3, we present the reconciliation approaches that we consider in this study, including the new aggregated-down approach and their simplified formulas according to the specific hierarchical structure of aggregated curves. Furthermore, we show that under some assumptions, the reconciliation approach is independent of the previously introduced curve representations. In Section 4, we present a simulation study of the new aggregated-down approach where we analyze and compare with the other reconciliation methods considered in this study. In Section 5, we introduce the market clearing mechanism for the German day-ahead electricity market and the model used to forecast the day-ahead supply and demand curves. We also present our empirical study, the data used, and the empirical results. We summarize the results and provide our conclusions in Section 6.

2 Hierarchical structure of aggregated curves

The hierarchical structure of a curve can be represented in multiple ways, i.e. the relationship between the bottom-level or marginal values and the curve itself, or the aggregated values. The curve can be obtained from an aggregation procedure with the marginals. Alternatively, we can start with the curve and describe a disaggregation relationship to obtain the bottom values.

However, a natural method of representation that we refer to as the canonical structure of an aggregated curve is shown in Figure 2. At the end of this section, we also discuss other representations.

2.1 Canonical representation

The canonical representation of an aggregated curve as we illustrate in Figure 2 is regarded as the standard representation. This representation also appears naturally when modeling auction curves in economics [Ziel and Steinert, 2016]. It can be obtained by considering the bottom values together with an aggregation procedure to receive the aggregated values, but also the other way around.

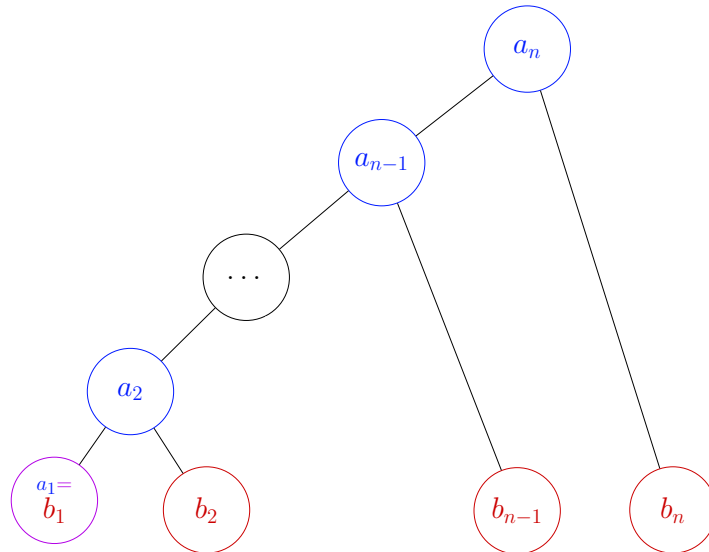


Figure 2: Hierarchical structure of an aggregated curve

Based on the first approach above, we introduce the following notation. Let $\mathbf{b} = (b_1, \dots, b_n)'$ be the n -dimensional vector of bottom-level or marginal values with $n > 1$,

as shown in Figure 2. Now, we introduce their aggregation by the vector $\mathbf{a} = (a_1, \dots, a_n)'$, which is an n -dimensional vector of aggregated or cumulative values starting from the top level, where a_i for $i \in \{1, \dots, n\}$ represents the curve at point i . Formally, this is defined as

$$a_i = \sum_{j=1}^i b_j, \quad (1)$$

i.e. the cumulative sum of \mathbf{b} . In addition, the recursive relationship holds

$$a_i = a_{i-1} + b_i \text{ for } 1 \leq i < n \text{ and } a_1 = b_1. \quad (2)$$

We note that Equation (2) is simply the mathematical representation of Figure 2. The top level a_n is the most aggregated level.

Alternatively, we can introduce the canonical representation starting from the aggregated values \mathbf{a} . Then, we can obtain the bottom values \mathbf{b} by disaggregation or differencing with an initial value for b_1 :

$$b_i = a_i - a_{i-1}, \text{ for } 1 < i \leq n \text{ and } b_1 = a_1. \quad (3)$$

Furthermore, we can express \mathbf{b} as $\mathbf{b} = \mathbf{D}\mathbf{a}$ where \mathbf{D} is an invertible n -dimensional quadratic matrix defined as

$$\mathbf{D}_n = \begin{bmatrix} 1 & 0 & \dots & 0 & 0 \\ -1 & 1 & \dots & 0 & 0 \\ \vdots & \vdots & \ddots & \vdots & \vdots \\ 0 & 0 & \dots & -1 & 1 \end{bmatrix}. \quad (4)$$

Consequently, the matrix representation of equation (1) is $\mathbf{a} = \mathbf{D}_n^{-1}\mathbf{b}$ where \mathbf{D}_n^{-1} is a lower-left triangular matrix with ones on the diagonal and lower triangle. Using the definitions of aggregated values \mathbf{a} and bottom-level values \mathbf{b} we can compactly write all of the values shown in Figure (2) as the $(2n - 1)$ -dimensional vector

$$\mathbf{y} = \begin{bmatrix} a_n \\ \vdots \\ a_2 \\ \mathbf{b} \end{bmatrix} \quad (5)$$

which contains the values of \mathbf{a} in inverse order except for its first value a_1 , which matches b_1 . Thus, $(y_1, \dots, y_n)'$ may be regarded as aggregated values and $(y_n, \dots, y_{2n-1})'$ as bottom-level values.

The aggregation relationship within \mathbf{y} can be represented using the $(2n - 1) \times n$ -dimensional summation matrix \mathbf{S} , which describes the hierarchical structure of the considered data such that $\mathbf{y} = \mathbf{S}\mathbf{b}$ holds. For the considered canonical representation we have

$$\mathbf{S} = \left[\begin{array}{c|c} \mathbf{1}_{n-1} & \mathbf{U}_{n-1} \\ \hline & \mathbf{I}_n \end{array} \right] = \left[\begin{array}{cccccc} 1 & 1 & \cdots & 1 & 1 \\ 1 & 1 & \cdots & 1 & 0 \\ \vdots & \vdots & \ddots & \vdots & \vdots \\ 1 & 1 & \cdots & 0 & 0 \\ \hline 1 & 0 & \cdots & 0 & 0 \\ 0 & 1 & \cdots & 0 & 0 \\ \vdots & \vdots & \ddots & \vdots & \vdots \\ 0 & 0 & \cdots & 1 & 0 \\ 0 & 0 & \cdots & 0 & 1 \end{array} \right], \quad (6)$$

where \mathbf{U}_{n-1} is a unit anti-diagonal upper-left triangular matrix of dimension $(n - 1)$ and \mathbf{I}_n is an identity matrix of dimension n .

Other situations can be considered where even more parts of the hierarchical curve are available. Using the notation $b_{i:j} = \sum_{l=i}^j b_l$ the canonical setting uses $b_{1:j}$ for $j > 1$ for the aggregated values, i.e. $\mathbf{a} = (b_{1:1}, b_{1:2}, \dots, b_{1:n})'$. We could also consider a setting where, e.g. $b_{2:3} = b_2 + b_3$, is also available, which would enrich the hierarchical structure with this additional information. However, the resulting structures that include general $b_{i:j}$ combinations could include up to $n(n - 1)/2$ values in the corresponding \mathbf{y} vector. This would increase computational costs substantially, so we only study the specific structure where forecasts $\hat{\mathbf{y}}$ (or equivalently $\hat{\mathbf{a}}$ and $\hat{\mathbf{b}}$) are available to the forecaster.

2.2 Other representations of aggregated curves

In this subsection, we discuss representations other than the canonical one for aggregated curves. We generalize the representation scheme so the canonical representation is embedded. In particular, we consider a situation where the aggregated values \mathbf{a} are given and the scope involves defining a disaggregation rule to receive the bottom values \mathbf{b} .

We introduce k as the element of \mathbf{a} where from we start the disaggregation rule. In the canonical representation we disaggregate \mathbf{a} starting from the first value $k = 1$ of the curve, i.e. for $k = 1$ it holds that $b_k = a_k$, $b_i = a_i - a_{i-1}$ for $i > k$ (see Equation (3)). This starting point of aggregation/disaggregation k could be changed to achieve an alternative

	i	1	2	3	4	5	6
\mathbf{a}	a_i	1	4	6	7	10	15
$\mathbf{b}_{[1]}$	$b_{[1],i}$	1	3	2	1	3	5
$\mathbf{b}_{[3]}$	$b_{[3],i}$	-3	-2	6	1	3	5
$\mathbf{b}_{[6]}$	$b_{[6],i}$	-3	-2	-1	-3	-5	15

Table 1: Different disaggregation results for $k = 1, 3, 6$ and a specific \mathbf{a} of length $n = 6$.

bottom-values vector $\mathbf{b}_{[k]}$. Clearly, $\mathbf{b} = \mathbf{b}_{[1]}$ and if we start disaggregating from the end, i.e. $k = n$, we obtain $b_{[n],1} = a_n$, $b_{[n],2} = a_{n-1} - a_n$, and in general, $b_{[n],i} = a_{n-i+1} - a_{n-i+2}$. Thus, $b_{[n],i}$ has the opposite sign to b_i for $i < n$. However, this approach can be embedded in the canonical representation, which we receive by defining $b_i = b_{[n],n-i+1}$. Thus, the theory of canonical representations can also be applied.

If we consider the disaggregation procedure with an initial value at k where $1 < k < n$ with the corresponding value $b_{[k],k} = a_k$, then we obtain a representation that is substantially different from the $\mathbf{b}_{[1]}$ and $\mathbf{b}_{[n]}$ situations. The reason for this difference is that we require two directions of aggregation, with one for bottom values larger than k and the other one for smaller values. Thus, we have

$$b_{[k],i} = \begin{cases} a_i - a_{i-1} & , \text{ if } i > k \\ a_i - a_{i+1} & , \text{ if } i < k \\ a_i & , \text{ if } i = k \end{cases} \quad (7)$$

We observe that the special cases of $\mathbf{b}_{[1]}$ (the canonical representation) and $\mathbf{b}_{[n]}$ can be defined using the definition (7). For illustrative purposes and to easier understand, we provide an $n = 6$ -dimensional example for $k = 1, 3, 6$ in Table 1.

In the general $\mathbf{b}_{[k]}$ setting, the summation matrix $\mathbf{S}_{[k]}$ is given by

$$\mathbf{S}_{[k]} = \begin{bmatrix} \mathbf{O}_{n-k,k-1} & \mathbf{1}_{n-k} & \mathbf{U}_{n-k} \\ \mathbf{L}_{k-1} & \mathbf{1}_{k-1} & \mathbf{O}_{k-1,n-k} \\ \mathbf{I}_n \end{bmatrix} \quad (8)$$

where \mathbf{L}_{k-1} is a $(k-1)$ -dimensional matrix that contains 1 on the lower anti-diagonal. The general summation matrix $\mathbf{S}_{[k]}$ in (8) also nests the canonical case \mathbf{S} in (6) for $k = 1$. The

vector $\mathbf{y}_{[k]}$ in the corresponding hierarchy that satisfies $\mathbf{y}_{[k]} = \mathbf{S}_{[k]}\mathbf{b}$ is

$$\mathbf{y}_{[k]} = \begin{bmatrix} \mathbf{a}_{[-k]} \\ \mathbf{b}_{[k]} \end{bmatrix} \quad (9)$$

where we define $\mathbf{a}_{[-k]}$ as the reversed vector \mathbf{a} without the k th element, i.e. $\mathbf{a}_{[-k]} = (a_n, \dots, a_{k+1}, a_{k-1}, \dots, a_1)'$. Clearly, for $k = 1$ we have $\mathbf{y} = \mathbf{y}_{[k]}$ (see definition (9)).

However, the different representations of the hierarchical structure are actually only formal representations and do not automatically provide different reconciled forecasts by themselves, as shown at the end of the next section. To show that this is the case, we observe that the following relations hold:

$$a_i = \begin{cases} \sum_{j=k}^i b_{[k],j} & , \text{ if } i > k \\ \sum_{j=i}^k b_{[k],j} & , \text{ if } i \leq k \end{cases} \quad (10)$$

and

$$b_i = \begin{cases} a_1 & , \text{ if } i = 1 \\ -b_{[k],i-1} & , \text{ if } 1 < i < k + 1 \\ b_{[k],i} & , \text{ if } i \geq k + 1. \end{cases} \quad (11)$$

These relations help us define Equation (7) in matrix form as $\mathbf{b}_{[k]} = \mathbf{A}_{[k]}\mathbf{a}$ with matrix $\mathbf{A}_{[k]}$, which yields $\mathbf{y}_{[k]} = \mathbf{S}_{[k]}\mathbf{A}_{[k]}\mathbf{a}$. For $k = 1$, we have $\mathbf{A}_{[k]} = \mathbf{D}_n$ from Equation (4). $\mathbf{A}_{[k]}$ has the form:

$$\mathbf{A}_{[k]} = \begin{bmatrix} \mathbf{I}_{k-1} + \begin{bmatrix} \mathbf{0}_{k-2+1} & -\mathbf{I}_{k-2} \\ 0 & \mathbf{0}'_{k-2+1} \end{bmatrix} & \begin{bmatrix} \mathbf{0}_{k-2} \\ -1 \end{bmatrix} & & \mathbf{0}_{k-1,n-k} \\ \mathbf{0}'_{k-1} & 1 & & \mathbf{0}'_{n-k} \\ \mathbf{0}_{n-k,k-1} & \begin{bmatrix} -1 \\ \mathbf{0}_{n-k-1} \end{bmatrix} & \mathbf{I}_{n-k} + \begin{bmatrix} \mathbf{0}_{n-k-1} & 0 \\ -\mathbf{I}_{n-k-1} & \mathbf{0}'_{n-k-1} \end{bmatrix} \end{bmatrix}. \quad (12)$$

In addition, according to definition (9), a matrix $\mathbf{B}_{[k]}$ exists that satisfies $\mathbf{y} = \mathbf{B}_{[k]}\mathbf{y}_{[k]}$. We note that $\mathbf{B}_{[k]}$ has the structure

$$\mathbf{B}_{[k]} = \begin{bmatrix} \mathbf{I}_{n-k} & \mathbf{0}_{n-k,k-1} & \mathbf{0}_{n-k,k-1} & \mathbf{0}_{n-k} & \mathbf{0}_{n-k,n-k} \\ \mathbf{0}'_{n-k} & \mathbf{0}'_{k-1} & \mathbf{0}'_{k-1} & 1 & \mathbf{0}'_{n-k} \\ \mathbf{0}_{k-1,n-k} & \mathbf{I}_{k-1} & \mathbf{0}_{k-1,k-1} & \mathbf{0}_{k-1} & \mathbf{0}_{k-1,n-k} \\ \mathbf{0}_{k-1,n-k} & \mathbf{0}_{k-1,k-1} & -\mathbf{I}_{k-1} & \mathbf{0}_{k-1} & \mathbf{0}_{k-1,n-k} \\ \mathbf{0}_{n-k,n-k} & \mathbf{0}_{n-k,k-1} & \mathbf{0}_{n-k,k-1} & \mathbf{0}_{n-k} & \mathbf{I}_{n-k} \end{bmatrix}. \quad (13)$$

Furthermore, it is easy to check that $\mathbf{B}_{[k]}$ is orthogonal, i.e. it holds $\mathbf{B}_{[k]}^{-1} = \mathbf{B}'_{[k]}$. We observe that $\mathbf{B}_{[k]}$ is a generalized permutation matrix that contains permutations and reflection components.

Finally, using $\mathbf{y} = \mathbf{B}_{[k]}\mathbf{y}_{[k]}$, $\mathbf{y}_{[k]} = \mathbf{S}_{[k]}\mathbf{A}_{[k]}\mathbf{a}$ and $\mathbf{a} = \mathbf{D}_n^{-1}\mathbf{b}$ we obtain that $\mathbf{y} = \mathbf{B}_{[k]}\mathbf{S}_{[k]}\mathbf{A}_{[k]}\mathbf{D}_n^{-1}\mathbf{b}$. Thus, it holds that $\mathbf{S} = \mathbf{B}_{[k]}\mathbf{S}_{[k]}\mathbf{A}_{[k]}\mathbf{D}_n^{-1}$ for all k , which is valuable for further analysis.

3 Reconciliation approaches

In general, the hierarchical structure does not hold if each time series is forecasted individually. As stated by Wickramasuriya et al. [2019], we call these individual forecasts incoherent or base forecasts, and denote them by $\hat{\mathbf{y}}$. The coherent or reconciled forecasts for which the structure in Figure 2 holds are denoted by $\tilde{\mathbf{y}}$, and they formally satisfy: $\tilde{\mathbf{y}} = \mathbf{S}\tilde{\mathbf{b}}$, where $\tilde{\mathbf{b}}$ are the bottom values in $\tilde{\mathbf{y}}$.

The coherency of forecasts is a desired property of aggregated curves for further analysis, e.g. for trading applications, but the main application of reconciliation is generating accurate values for the aggregated level \mathbf{a} . All linear reconciliation approaches for any hierarchical structure can be compactly written in matrix notation as

$$\tilde{\mathbf{y}} = \mathbf{S}\mathbf{P}\hat{\mathbf{y}} \tag{14}$$

The $(2n - 1) \times n$ -dimensional mapping matrix \mathbf{P} maps the base forecasts \mathbf{y} to the bottom level, [Hyndman and Athanasopoulos, 2018]. \mathbf{P} is different for each reconciliation approach. The product $\mathbf{S}\mathbf{P}$ is sometimes referred to as the reconciliation or projection matrix.

In the previous section, we described the canonical representation and other representations. We note that they imply the same hierarchical structure and it holds that $\mathbf{S} = \mathbf{B}_{[k]}\mathbf{S}_{[k]}\mathbf{A}_{[k]}\mathbf{D}_n^{-1}$. Furthermore, the results are actually equivalent for specific reconciliation approaches considered in the simulation study and application, i.e. they are not affected by the choice of k (see Section (3.4) for more details). Therefore, in the following subsections, we only consider the canonical representation.

3.1 Simple benchmark approaches

Table 2 summarizes the formulas for our three benchmark reconciliation approaches: bottom-up, top-down and aggregated-down. The first two approaches are well-established proce-

dures, so we will not provide their details but instead we refer to previous studies (Hyndman and Athanasopoulos [2018], Gross and Sohl [1990]). For the top-down and aggregated down methods, we provide three options for calculating the disaggregating proportions, i.e., using the average ratio (ar), ratio of averages (ra), and forecasted values (fo). Many more options could be considered for the top-down approach (Gross and Sohl [1990]). We describe the new aggregated-down approach in the next subsection.

Method	Mapping matrix \mathbf{P}
Bottom-up	$\mathbf{P}_{\text{bu}} = \begin{bmatrix} \mathbf{O}_{n \times (n-1)} & \mathbf{I}_n \end{bmatrix}$
Top-down	$\mathbf{P}_{\text{td}} = \begin{bmatrix} \mathbf{p} & \mathbf{O}_{n \times (2n-2)} \end{bmatrix}$ $\mathbf{p} = (p_1, \dots, p_n)'$ Average ratio: $\hat{p}_{\text{ar},j} = \frac{1}{T} \sum_{t=1}^T \frac{b_{j,t}}{a_{n,t}}$ Ratio of averages: $\hat{p}_{\text{ra},j} = \frac{\frac{1}{T} \sum_{t=1}^T b_{j,t}}{\frac{1}{T} \sum_{t=1}^T a_{n,t}}$ Forecasted values: $\hat{p}_{\text{fo},j} = \begin{cases} \frac{\hat{b}_n}{\hat{a}_{n-1} + \hat{b}_n}, & \text{for } j = n \\ \frac{\hat{b}_j}{\hat{a}_{j-1} + \hat{b}_j} \prod_{i=j}^{n-1} \left(\frac{\hat{a}_i}{\hat{a}_i + \hat{b}_{i+1}} \right) & \text{for } 1 < j < n, \\ \prod_{i=1}^{n-1} \left(\frac{\hat{a}_i}{\hat{a}_i + \hat{b}_{i+1}} \right) & \text{for } j = 1. \end{cases}$
Aggregated-down	$\mathbf{P}_{\text{ad}} = \begin{bmatrix} \mathbf{Q}_{n \times n} & \mathbf{O}_{n \times (n-1)} \end{bmatrix}$ $\mathbf{Q}_{n \times n} = \text{Antidiag}(\mathbf{q}) = \text{Antidiag}((q_1, \dots, q_n)')$ $q_1 = 1$ Average ratio: $\hat{q}_{\text{ar},j} = \frac{1}{T} \sum_{t=1}^T \frac{a_{j,t} - a_{j-1,t}}{a_{j,t}} = \frac{1}{T} \sum_{t=1}^T \frac{b_{j,t}}{a_{j,t}}$ Ratio of averages: $\hat{q}_{\text{ra},j} = \frac{\frac{1}{T} \sum_{t=1}^T a_{j,t} - a_{j-1,t}}{\frac{1}{T} \sum_{t=1}^T a_{j,t}} = \frac{\frac{1}{T} \sum_{t=1}^T b_{j,t}}{\frac{1}{T} \sum_{t=1}^T a_{j,t}}$ Forecasted values: $\hat{q}_{\text{fo},j} = \frac{\hat{a}_j - \hat{a}_{j-1}}{\hat{a}_j}$ for $j > 1$,

Table 2: Reconciliation methods and their formulas for aggregated curves (\mathbf{O}_{\times} is a zero matrix of indicated dimensions)

We use *bu* as an abbreviation for bottom-up, and *tdar*, *tdra*, *tdfo* for the top-down approaches using the average ratio, the ratio of averages, and forecasted values respectively.

3.2 Aggregated-down approach

The aggregated-down approach is essentially a localized top-down approach, where the disaggregating proportions are calculated based on the node above and not based on the top-

most aggregated level. The motivation for this approach is based on the simple assumption that proportions calculated using values that are closer in the hierarchical structure are expected to be more accurate than when using values that are further away. We provide support for this assumption based on our simulation study in the next section.

We denote the corresponding disaggregating proportions by q_j where $\mathbf{q} = (q_1, \dots, q_n)'$ is the vector of proportions. By design (see Fig. 2), it holds that

$$b_j = q_j a_{n-j+1}. \quad (15)$$

Thus, q_j is the disaggregation proportion for b_j given a_{n-j+1} at the corresponding connection of the tree. The mapping matrix is defined as

$$\mathbf{P}_{\text{ad}} = \begin{bmatrix} \mathbf{Q} & \mathbf{O}_{n \times (n-1)} \end{bmatrix},$$

where $\mathbf{Q} = \text{Antidiag}(\mathbf{q})$ is a $n \times n$ anti-diagonal matrix with the elements on the anti-diagonal starting from top to bottom, i.e.,

$$\mathbf{Q} = \begin{bmatrix} 0 & \dots & 0 & q_1 \\ 0 & \dots & q_2 & 0 \\ \vdots & \vdots & \ddots & \vdots \\ q_n & 0 & \dots & 0 \end{bmatrix}.$$

We require that $q_1 = 1$ every time, which corresponds to $\tilde{b}_1 = \hat{b}_1$. Analogous to the top-down approach, the proportions can be estimated using various methods, which are summarized in Table 2. It should be noted that the methods for calculating the average ratio and ratio of averages proportion calculation methods have similar complexity for the top-down and aggregated-down approaches. However, the formula for calculating the aggregated-down approach using the forecasted values $\hat{\mathbf{y}}$ is much simpler than that for the top-down approach.

We use *adar*, *adra*, *adfo* as abbreviations for the aggregated-down approaches using the average ratio, the ratio of averages, and forecasted values, respectively (see Table 2).

3.3 Optimal reconciliation approach

Hyndman and Athanasopoulos [2018] and Wickramasuriya et al. [2019] introduced the optimal reconciliation approach by showing that the optimal mapping matrix that obtains

the best, unbiased coherent forecasts is given by

$$\mathbf{P}_{\text{op}} = (\mathbf{S}'\mathbf{W}^{-1}\mathbf{S})^{-1}\mathbf{S}'\mathbf{W}^{-1} \quad (16)$$

where $\mathbf{W} = \text{Var}[\mathbf{y} - \hat{\mathbf{y}}]$ is the variance-covariance matrix of the base forecast errors. Equation (16) is the result obtained by minimizing the variance of the coherent forecasts. \mathbf{W} is not known and must be estimated. We consider multiple estimators for \mathbf{W} , which are listed below. The first five estimators were proposed by Hyndman and Athanasopoulos [2018] and Wickramasuriya et al. [2019].

1. $\mathbf{W}_{\text{opols}} = \mathbf{I}_{2n-1}$, where \mathbf{I}_{2n-1} is the identity matrix. For the optimal projection matrix \mathbf{P} in the aggregated curves setting, we have $\mathbf{P}_{\text{opols}} = (\mathbf{S}'\mathbf{S})^{-1}\mathbf{S}'$. We note that $\mathbf{S}'\mathbf{S}$ is of full rank and invertible because it holds

$$\mathbf{S}'\mathbf{S} = [\mathbf{1}_{n-1} : \mathbf{U}_{n-1}]'[\mathbf{1}_{n-1} : \mathbf{U}_{n-1}] + \mathbf{I}_n = \begin{bmatrix} n & n-1 & n-2 & \cdots & 2 & 1 \\ n-1 & n & n-2 & \cdots & 2 & 1 \\ n-2 & n-2 & n-1 & \cdots & 2 & 1 \\ \vdots & \vdots & \vdots & \ddots & \vdots & \vdots \\ 2 & 2 & 2 & \cdots & 3 & 1 \\ 1 & 1 & 1 & \cdots & 1 & 2 \end{bmatrix}.$$

Thus, we obtain $\mathbf{P}_{\text{opols}} = ([\mathbf{1}_{n-1} : \mathbf{U}_{n-1}]'[\mathbf{1}_{n-1} : \mathbf{U}_{n-1}] + \mathbf{I}_n)^{-1}\mathbf{S}'$. However, the assumption that $\text{Var}[\mathbf{y} - \hat{\mathbf{y}}]$ is constant is usually not realistic in an aggregated curve setting because we expect a tendency towards larger variances for higher aggregation levels. We use *opols* as an abbreviation for this approach.

2. $\mathbf{W}_{\text{oplambd}} = \mathbf{\Lambda}$, $\mathbf{\Lambda} = \text{Diag}(\mathbf{S}\mathbf{1}_n)$, where \mathbf{S} is the summation matrix and $\mathbf{1}_n$ is a unit vector of the same dimension as the number of bottom-level time series. In our aggregated curves setting, it holds that $\text{Diag}(\mathbf{\Lambda}) = \mathbf{S}\mathbf{1}_n = (n, n-1, \dots, 2, 1, 1, \dots, 1)'$, which means that the higher aggregated values of the curves are weighted less, proportional to their level of aggregation starting from 1 as the lowest and n as the top. This corresponds to a setting where all bottom-level forecasts \mathbf{b} have the same variance and are uncorrelated. We use *oplambd* as an abbreviation for this approach.
3. $\mathbf{W}_{\text{opwls}} = \widehat{\mathbf{W}}_{\text{dcov}}$, where $\widehat{\mathbf{W}}_{\text{dcov}}$ is an estimator for $\mathbf{W}_{\text{dcov}} = \text{Diag}(\mathbf{W}_{\text{cov}})$ with \mathbf{W}_{cov} as the covariance matrix of the errors associated with \mathbf{y} . \mathbf{W}_{cov} can be estimated by

the sample covariance $\widehat{\mathbf{W}}_{\text{cov}}$, i.e. $\widehat{\mathbf{W}}_{\text{cov}} = \frac{1}{n} \mathbf{E}' \mathbf{E} = \frac{1}{n} \sum_{i=1}^n \mathbf{e}_i \mathbf{e}_i'$ and \mathbf{E} is the matrix of residuals generated by and arranged in the same order as the base forecasts. The $\mathbf{W}_{\text{opwls}}$ approach may be regarded as a generalization of the $\mathbf{W}_{\text{oplambd}}$ approach. This design corresponds to a setting where the individual forecast errors have different variances but are uncorrelated. We use *opwls* as an abbreviation for this approach.

4. $\mathbf{W}_{\text{opcov}} = \widehat{\mathbf{W}}_{\text{cov}}$, where \mathbf{W}_{cov} is the full sample covariance matrix of the error terms. The underlying setting corresponds to a situation where the forecast errors have varying variances and exhibit linear dependence. We use *opcov* as an abbreviation for this approach.

5. $\mathbf{W}_{\text{opshrink}} = \lambda \widehat{\mathbf{W}}_{\text{dcov}} + (1 - \lambda) \widehat{\mathbf{W}}_{\text{cov}}$, where λ is the shrinkage intensity parameter. Schäfer and Strimmer [2005] proposed setting

$$\lambda = \frac{\sum_{i \neq j} \widehat{\text{Var}}(\widehat{r}_{ij})}{\sum_{i \neq j} \widehat{r}_{ij}^2},$$

where \widehat{r}_{ij} is the ij th element of the 1-step-ahead sample correlation matrix. The authors implemented the formulas in the `corpcor` R package. We use *opshrink* as an abbreviation for this approach.

6. Ledoit-Wolf covariance matrix estimator with shrinkage toward constant correlation [Ledoit and Wolf, 2004]: $\mathbf{W}_{\text{opledoitwolf}} = \delta \mathbf{F} + (1 - \delta) \widehat{\mathbf{W}}_{\text{cov}}$, where $\widehat{\mathbf{W}}_{\text{cov}}$ is the sample covariance matrix, \mathbf{F} is the shrinkage target with constant correlation defined with element $f_{ij} = \bar{r} \sqrt{\widehat{w}_{ii} \widehat{w}_{jj}}$ on the i th row and j th column, \widehat{w}_{ij} is the corresponding element of $\widehat{\mathbf{W}}_{\text{cov}}$, and

$$\bar{r} = \frac{2}{(N-1)N} \sum_{i=1}^{N-1} \sum_{j=i+1}^N r_{ij},$$

$r_{ij} = \frac{\widehat{w}_{ij}}{\sqrt{\widehat{w}_{ii} \widehat{w}_{jj}}}$. The estimator of the shrinkage intensity δ was introduced by [Ledoit and Wolf, 2004]. We use *opledoitwolf* as an abbreviation for this approach.

7. Covariance matrix estimation using graphical lasso [Friedman et al., 2008]:

$$\mathbf{W}_{\text{opglasso}} = \begin{bmatrix} \mathbf{W}_{11} & \mathbf{w}_{12} \\ \mathbf{w}'_{12} & w_{22} \end{bmatrix},$$

where $\mathbf{W}_{\text{opglasso}}$ is partitioned as shown and estimated by using coordinated descent to solve

$$\boldsymbol{\beta}_{\text{opglasso}} = \arg \min_{\boldsymbol{\beta}} \left\{ \frac{1}{2} \|\mathbf{W}_{11}^{1/2} \boldsymbol{\beta} - \mathbf{b}\|^2 + \rho \|\boldsymbol{\beta}\|_1 \right\},$$

where $\mathbf{b} = \mathbf{W}_{11}^{-1/2} \hat{\mathbf{w}}_{12}$. The optimal $\boldsymbol{\beta}$ is used to generate the optimal $\mathbf{w}_{12} = \mathbf{W}_{11} \boldsymbol{\beta}_{\text{opglasso}}$. Initially, $\mathbf{W}_{\text{opglasso}}$ is set to $\mathbf{W} = \widehat{\mathbf{W}}_{\text{cov}} + \rho \mathbf{I}_n$. We used the algorithm as implemented by [Friedman et al., 2008] in the `glasso` R package. We use *opglasso* as an abbreviation for this approach.

3.4 Optimal reconciliation for other representations

Next, we briefly describe the optimal reconciliation approach for other representations. In this situation, for some k , we have

$$\tilde{\mathbf{P}}_{[k]} = (\mathbf{S}'_{[k]} \mathbf{W}_{[k]}^{-1} \mathbf{S}_{[k]})^{-1} \mathbf{S}'_{[k]} \mathbf{W}_{[k]}^{-1}.$$

Furthermore, we can show that under mild assumptions regarding the forecast method and the reconciling matrix $\mathbf{W}_{[k]}$, the reconciliation approach preserves the hierarchical structure, which holds in the sense that the result does not depend on the choice of k :

Theorem 1. *If $\hat{\mathbf{y}} = \mathbf{B}_{[k]} \hat{\mathbf{y}}_{[k]}$ and $\mathbf{W}_{[k]}^{-1} = \mathbf{B}'_{[k]} \mathbf{W}^{-1} \mathbf{B}_{[k]}$ then it holds that*

$$\tilde{\mathbf{y}} = \mathbf{B}_{[k]} \tilde{\mathbf{y}}_{[k]}.$$

The proof is presented in the Appendix. We recall that $\mathbf{B}_{[k]}$ is orthogonal, and thus the assumption $\hat{\mathbf{y}} = \mathbf{B}_{[k]} \hat{\mathbf{y}}_{[k]}$ is satisfied if the forecasting algorithm that provides $\hat{\mathbf{y}}$ is invariant to orthogonal transformations, e.g., this holds for linear regressions. In addition, we note that $\mathbf{W}_{[k]}^{-1} = \mathbf{B}'_{[k]} \mathbf{W}^{-1} \mathbf{B}_{[k]}$ is trivially satisfied if $\mathbf{W} = \mathbf{I}_{2n-1}$ due to orthogonality of $\mathbf{B}_{[k]}$.

4 Simulation study

The new aggregated-down approach is motivated based on the simple idea of closeness, i.e. proportions calculated using values that are closer in the hierarchical structure are expected to be more accurate than those calculated when using values that are further away due to avoidance of error aggregation. To support this claim, we conducted a simulation study, which also allowed us to compare the performance with other approaches.

4.1 Study design

Number of historical observations (N)	$N \in \{16, 64, 256\}$
Number of bottom-level values (n)	$n \in \{4, 16, 64\}$
Coefficient matrix (Φ)	$\Phi = a\mathbf{I}_n$ for $a \in \{0.2, 0.5, 0.7, 0.95\}$
Error variance-covariance matrix (A)	$A = \mathbf{I}_n$

Table 3: Simulation study setup: combinations for a VAR(1) process.

We simulated Vector Auto-Regressive VAR(1) processes for the bottom-level values. We replicated the simulation 1000 times for each combination of the parameters specified in Table 3.

We also considered the case of correlated errors with the variance-covariance matrix $A = 0.3\mathbf{I}_n + 0.7\mathbf{1}\mathbf{1}'$ in combination with the coefficient matrix $\Phi = 0.7\mathbf{I}_n$. We generated the aggregated values from the bottom-level simulations and fitted an Auto-Regressive AR(1) process without intercept for each level of the hierarchy. We calculated the forecast accuracy from 1-step-ahead forecasts for each level. Next, we computed the root mean square errors (RMSE) value of each reconciling approach considered.

4.2 Study results

The results are shown in Table 4 for the setup with $\Phi = 0.7\mathbf{I}_n$ and $A = \mathbf{I}_n$. We left out the results for the average ratio and ratio of averages approaches for top-down and aggregated-down since they were always greatly inferior to those obtained using the base case. We also omit some optimal methods for brevity because these tended to produce very similar results.

No. of bottom-level values (n)	4			16			64		
No. of observations (N)	16	64	256	16	64	256	16	64	256
base	1.40	1.39	1.32	2.24	2.27	2.24	4.33	4.13	4.15
bu	1.40	1.39	1.32	2.25	2.26	2.24	4.32	4.12	4.15
tdfo	18.0	8.07	1.61	55.7	99.5	74.1	24200	1610	605
adfo	1.42	1.39	1.32	2.26	2.27	2.24	4.35	4.13	4.15
opols	1.39	1.39	1.32	2.23	2.27	2.24	4.33	4.12	4.15
opwls	1.39	1.39	1.32	2.22	2.26	2.24	4.30	4.12	4.15
oplambd	1.39	1.39	1.32	2.21	2.26	2.24	4.29	4.12	4.15
opshrink	1.39	1.39	1.32	2.23	2.27	2.24	4.35	4.13	4.15

Table 4: Simulation study RMSE results for the VAR(1) setup $\Phi = 0.7\mathbf{I}_n$ and $A = \mathbf{I}_n$ for selected reconciliation methods

The key finding from this simulation study is that the aggregated-down approach using forecasted values was very similar to the other methods, and even optimal ones. By contrast, the top-down approach using forecasted values was markedly inferior in the setups considered. As expected, the accuracy generally decreases as more bottom-levels (n) were added. However, this was disproportionately the case with the top-down approach, which was caused by extreme sensitivity to outliers because the proportions were multiplicatively connected and common factors were present across the hierarchy. We refer to this issue as the *error inheritance* of proportions.

This situation is clear when we consider the formulas. For illustrative purposes, we consider the simplest proportions $\hat{p}_{fo,n}$, and $\hat{p}_{fo,n-1}$:

$$\hat{p}_{fo,n} = \frac{\hat{b}_n}{\hat{a}_{n-1} + \hat{b}_n}, \quad \hat{p}_{fo,n-1} = \frac{\hat{b}_{n-1}}{\hat{a}_{n-2} + \hat{b}_{n-1}} \underbrace{\frac{\hat{a}_{n-1}}{\hat{a}_{n-1} + \hat{b}_n}}_{=1-\hat{p}_{fo,n}}$$

Clearly, the formulas are sensitive to outliers when the denominator $\hat{a}_{n-1} + \hat{b}_n$ is very small, i.e. when $\hat{a}_{n-1} \approx -\hat{b}_n$. If this is the case, then all of the subsequent proportions will generally be outliers because $\hat{p}_{fo,n}$ is part of $\hat{p}_{fo,n-1}$, and so on. It should be noted that this occurs if we allow negative values. If we only consider monotonously increasing curves, then these outliers do not occur, as shown in Table 6, where we simulated a strictly positive AR(1) process leading to errors close to the other methods. To understand the sensitivity to outliers, Table 7 shows the results for the same setup with all outliers defined as $|\hat{p}_{fo,1}| > 50$ removed. The errors improved for greatly *tdfo*, especially with increasing values of N .

This issue is essentially error aggregation and is important considering the specific hierarchical structure of aggregated curves because the hierarchy considered is completely vertical and each additional point on the curve deepens the hierarchy instead of widening it. Thus, if we allow for negative values, the outliers become larger for *tdfo* when the hierarchy is deeper. The aggregated-down approach is not sensitive to this distance issue since proportions are not multiplicative, but instead they are always calculated using values immediately above the hierarchy level considered, and non-monotonic curves can be easily accommodated. The other simulation setups yielded similar results, as shown in Appendix Tables 8, 9, 10, and 11.

It is important to note that we consider the aggregated-down approach as a simple benchmark approach. It is not equivalent to more sophisticated optimal reconciliation

methods. Nevertheless, aggregated-down has the advantages of being intuitive and using very simple formulas for calculating proportion, especially compared to the top-down approaches, and is programmatically simple as well as efficient. Furthermore, it is not affected by the error aggregating issue, unlike the top-down approach.

5 Application

5.1 Supply and demand curves on day-ahead electricity markets

The European day-ahead electricity market is a daily, blind auction market where electricity prices are determined for each hour of the next day. The auction closes at 12:00 CET each day until when the market participants, i.e. the buyers and sellers, can submit buy (bid) and sell (ask) orders for each hour of the next day. These bids are the volumes that buyers are willing to buy and that producers are willing to sell at certain prices. For the time range of data considered, bid volumes can be specified for prices ranging from -500 EUR/MWh up to 3000 EUR/MWh with an increment of 0.1 EUR/MWh¹. After gate closure, the volumes bid across all participating countries are aggregated and unique prices and volumes are generated for each separate market area. One of these areas is Germany-Luxembourg, which we modeled and forecasted in this study. The market clearing results as well as the 24 supply and demand curves are published shortly after gate closure at 12:00 CET. All major relevant aspects of the German day-ahead electricity market are illustrated in Figure 3 (see Petropoulos et al. [2022] for more details). Only selected prices can be bid on out of a total of 35001 possible prices, so the curves have a characteristic step-like appearance due to the many zero-volume prices, i.e. prices that were not bid on Ziel and Steinert [2016].

Figure 4 shows the German volumes bid for each price for a selected day and hour. In total, there are 35001 prices that can be bid on for each hour, where most usually have a volume of zero, as can be observed by the many empty intervals between the bars. Certain prices are generally preferred by market participants, such as multiples of 10 and those in the vicinity of 40 EUR/MWh, as shown by the clusters formed around these prices in Figure 4. The hourly bids are aggregated to produce the day-ahead supply and demand curves for each hour, as shown in Figure 5.

¹Since 2022-05-11 the upper price limit was increased to 4000 EUR/MWh.

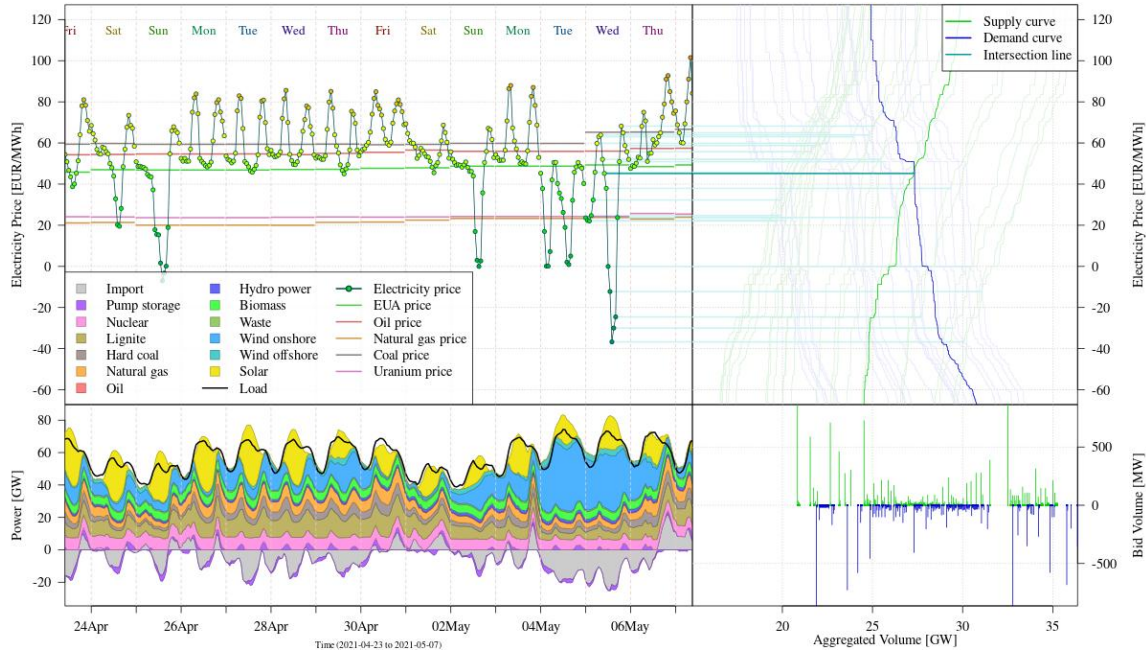
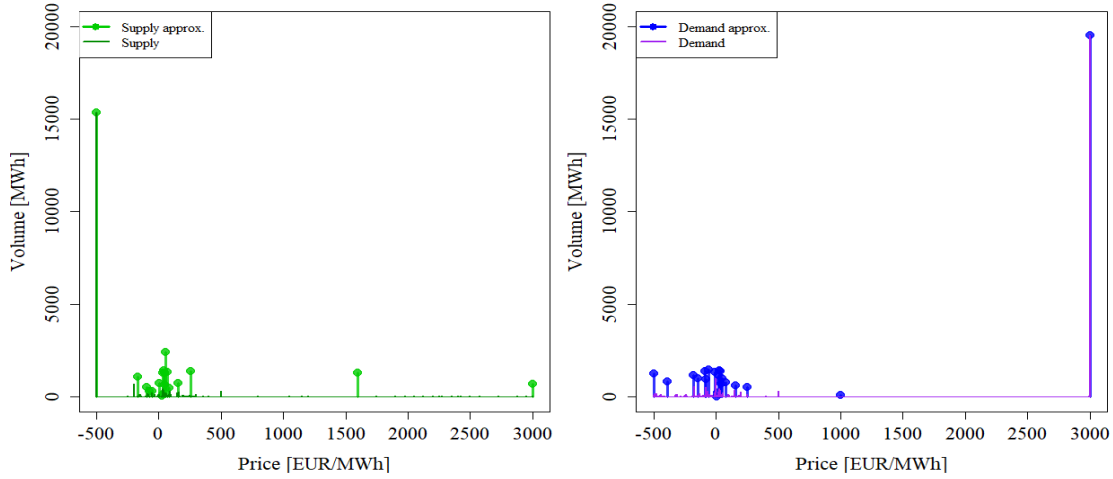


Figure 3: German-Luxembourg day-ahead market: Hourly day-ahead electricity price time series with relevant commodity price time series (top left) with corresponding 24 supply and demand curves on the price grid between -60 and 120 EUR/MWh for 5 May 2020 with highlighted curves for 11:00 (top right), power generation, import and consumption time series (bottom left), and bid structure of 5 May 2020 11:00 (bottom right).

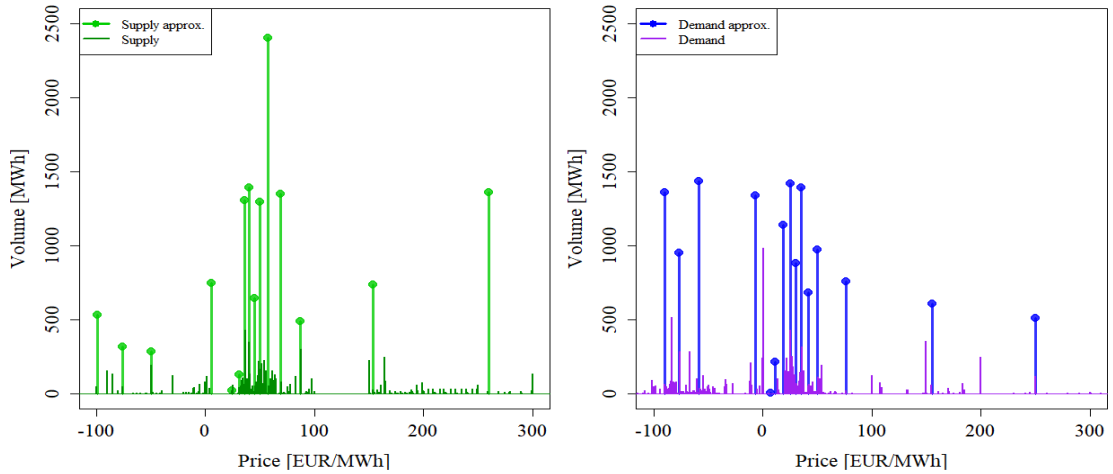
5.2 The X-Model

The X-Model introduced by [Ziel and Steinert, 2016] is an approach for forecasting day-ahead electricity prices as the intersection of supply and demand curves. The electricity prices are not modeled directly but instead they are obtained from the forecasts of the whole day-ahead curves as their intersection.

[Ziel and Steinert, 2016, 2018, Haben et al., 2021a, Kulakov, 2020] modeled the day-ahead supply and demand curves by grouping the prices into price classes, thus drastically reducing the dimensionality, e.g., from 350001 prices to a few price classes (40 in our study), to make the problem computationally feasible. The prices are split into price classes by inverting the supply and demand curves at a pre-specified grid of equidistant volumes [Ziel and Steinert, 2016]. The result is shown in Figure 5, where the curves are approximated by ca. 20 points each. This form of dimensionality reduction via binning can



(a) Volumes bid on all prices



(b) Volumes bid on selected price range

Figure 4: Volume bid per price for 2019-03-01 12:00:00, i.e. marginal values of the Supply and Demand curves. Volumes bid per price class are also shown, i.e. the marginal values of the Supply and Demand approximations. The bottom plots represent a magnification around 0.

be interpreted as a special case of applying FDA where the basis functions are constants, i.e. dummy variables, that do not overlap. This works very well in our case because the original curves are not smooth. An additional advantage is computability because it would be quite costly to smoothen the curves first, model them, and then un-smoothen them again for the final representation. [Ziel and Steinert, 2016] use a simple but very effective

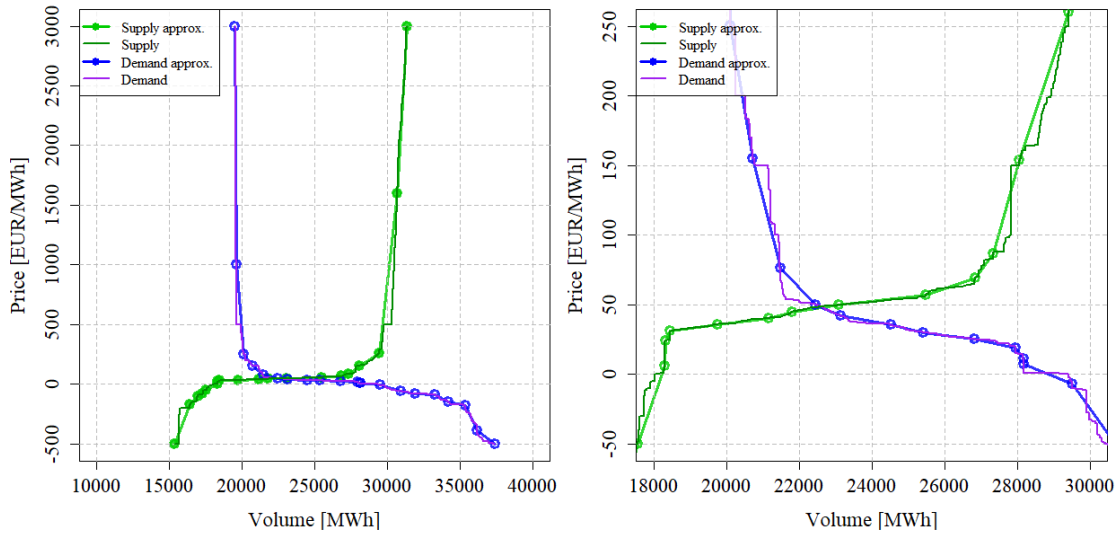


Figure 5: Supply and Demand curves for 2019-03-01 12:00:00, created by the cumulative aggregation of marginal volumes from Figure 4. Approximations of the Supply and Demand curves, created by cumulative aggregation of the price classes, are also shown. The plot on the right represents a magnification around the intersection point.

method for reconstructing the forecasted curves from the price class approximations, i.e., by using historical proportions for each price. This method was shown to capture the shape of the original curves very well without requiring vast computational resources. However, this reconstruction step is only important for calculating the price as the intersection of the supply and demand curves and does not affect the forecasting accuracy of the curves themselves, hence we refer to the original X-model paper for more information [Ziel and Steinert, 2016] as well as other papers that use more classical FDA approaches to implement the X-model [Soloviova and Vargiolu, 2021, Soloviova].

Thus, the response variable is the sum of the volume within a price class, which is modeled separately for every hour and class. For 40 price classes comprising both supply and demand, a total of 40×24 regressions must be conducted to forecast curves for all hours in the next day. [Ziel and Steinert, 2016] modeled each price class volume marginally, and thus the supply and demand curves were generated by cumulatively summing up the forecasted values, which is equivalent to forecasting only the bottom-level values and using the bottom-up reconciliation approach described earlier. In this study, we modeled both the marginal and cumulative responses, and used them to compare and contrast the different

reconciliation approaches. It should be noted that the method using marginal values will always be equivalent to the bottom-up approach.

To model the responses, we used a combination of autoregressive and external regressors. Let then $X_{S,d,h}^{(c)}$ and $X_{D,d,h}^{(c)}$ be the supply and demand volumes at day d and hour h of price class c among the price classes generated for the supply and demand curves, respectively. These constitute the bulk of the regressor matrix because each price class volume will depend on its lags according to a specific lag structure. The external regressors are denoted by $X_{X,d,h}^{(1)}, \dots, X_{X,d,h}^{(M_X)}$ for a total of M_X external regressors, and they comprise the prices for coal, gas, oil and CO₂ emissions (EUAs), the day-ahead prices and volumes on the previous day, as well as the day-ahead forecasts for the country-wide load, solar, onshore wind, and offshore wind production. The day-ahead data were taken from *www.epeixspot.com* and the forecasts from *www.entsoe.eu*.

Let M_S and M_D be the number of price classes for the supply and demand curves, respectively. Then, all regressors can be compactly written as

$$\mathbf{X}_{d,h} = (X_{1,d,h}, \dots, X_{M,d,h})' = \left(\left(X_{S,d,h}^{(c \in C_S)} \right), \left(X_{D,d,h}^{(c \in C_D)} \right), \left(X_{X,d,h}^{(c \in C_X)} \right) \right)',$$

where C_S and C_D are the sets of price classes for the supply and demand sides, respectively, C_X is the set of external regressors $C_X = \{X_{X,d,h}^{(1)}, \dots, X_{X,d,h}^{(M_X)}\}$, and $M = M_S + M_D + M_X$.

To capture the weekly seasonality, we also included dummy regressors for every day of the week which we denoted by a function $W_k(d)$ that returns the day of the week d . The full model can be written as

$$X_{m,d,h} = \sum_{k=1}^M \sum_{j=1}^{24} \sum_{l \in \mathcal{I}_{m,h}(l,j)} \phi_{m,h,l,j,k} X_{l,d-k,j} + \sum_{k=2}^7 \psi_{m,h,k} W_k(d) + \varepsilon_{m,d,h},$$

for $m \in \{1, \dots, M_S + M_D\}$ and $\mathcal{I}_{m,h}(l,j)$ represents the sets of possible lags, which we defined as

$$\mathcal{I}_{m,h}(l,j) = \begin{cases} \{1, \dots, 30\}, & \text{for } m = l \text{ and } h = j \\ \{1, \dots, 8\}, & \text{for } (m = l \text{ and } h \neq j) \text{ or } (m \neq l \text{ and } h = j) \\ \{1\}, & \text{for } m \neq l \text{ and } h \neq j \end{cases}.$$

We fitted the models using lasso [Ziel and Steinert, 2016] as implemented in the **glmnet** R package.

5.3 Data and results

We conducted a day-ahead rolling window forecasting study for each day between 2019-01-01 and 2019-06-30. We used a rolling window length of $730 = 2 \times 365$ days to forecast each day. The price classes were generated only once for the first day-ahead forecast, i.e. using the 2017 and 2018 data, and they were kept constant throughout the study. All data were hourly except for coal, gas, oil, and EUA prices, which were daily. We used marginal values as regressors to forecast the marginal values \hat{b}_i and cumulative values as regressors to forecast the cumulative values \hat{a}_i . We chose $\hat{a}_n \leftarrow \hat{b}_1$ for each day and hour, as in Figure 2.

To measure the forecasting accuracy, we used two popular error measures comprising the mean absolute errors (MAE) defined as

$$\text{MAE}_m^{\text{test}} = \frac{1}{24 \cdot \#(\mathcal{D})} \sum_{d \in \mathcal{D}} \sum_{h=0}^{23} |X_{m,d,h} - \hat{X}_{m,d,h}|$$

and the RMSE defined as

$$\text{RMSE}_m^{\text{test}} = \frac{1}{\#(\mathcal{D})} \sum_{d \in \mathcal{D}} \sqrt{\frac{1}{24} \sum_{h=0}^{23} (X_{m,d,h} - \hat{X}_{m,d,h})^2}$$

where \mathcal{D} is a set containing all 181 forecasted days, $\#(\cdot)$ is a function that returns the number of elements in a set, and $\hat{X}_{m,d,h}$ represents the respective forecasted value.

The averages over the MAEs and RMSEs for the overall price classes are shown in Figure 6. The top-down and aggregated-down approaches using historical proportions yielded worse results than the simple bottom-up method. Therefore, we do not include these results but they can be inspected in the comprehensive Tables 12 and 13. For the supply curve, the optimal lambda reconciliation approach obtained the smallest MAE on average, approximately 33 MWh lower than that with the marginal model. For the demand curve, the optimal shrinkage reconciliation approach returned the smallest MAE on average, approximately 97 MWh lower than that of with the marginal model. Similar results were obtained in terms of RMSEs, with differences of approx. 39 MWh and 109 MWh for the supply and demand curves respectively.

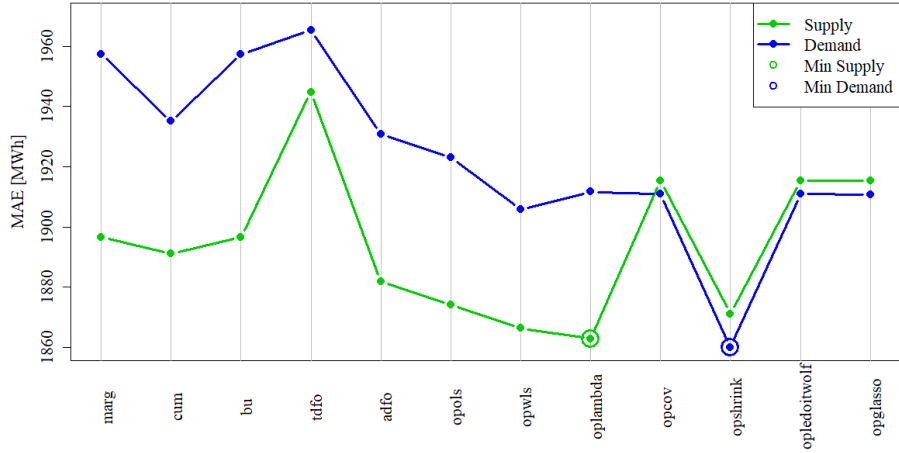
Table 5 shows the absolute MAE and percentage differences for some selected classes and the mean over all classes. Again, we do not include the results for the top-down and aggregated-down approaches using historical proportions for the same reasons stated

Price class:	Supply					Demand					Unit
	-500.0	-49.9	5.7	3000.0	Mean	3000.0	7.0	-6.9	-500.0	Mean	
marginal	1591	1827	1941	2087	1897	2051	1951	19664	1958	1957	MW
cumulative	-3.478	0.084	0.015	-0.584	-0.290	-2.540	0.907	1.307	2.689	-1.141	$\Delta\%$
bu	0.000	0.000	0.000	0.000	0.000	0.000	0.000	0.000	0.000	0.000	$\Delta\%$
tdfo	11.970	3.403	2.697	-0.940	2.536	-0.413	0.958	1.135	2.934	0.404	$\Delta\%$
adfo	0.000	-1.070	-1.059	-0.940	-0.780	0.000	0.398	0.850	2.934	-1.359	$\Delta\%$
opols	-0.472	-1.496	-1.667	-1.163	-1.183	-1.349	-0.409	-0.054	2.655	-1.756	$\Delta\%$
opwls	3.021	-1.684	-2.120	-2.607	-1.597	-2.860	-2.495	-2.379	1.053	-2.633	$\Delta\%$
oplambda	-0.207	-1.821	-2.115	-2.194	-1.782	-1.222	-2.075	-1.826	1.289	-2.336	$\Delta\%$
opcov	0.985	1.034	0.868	-0.011	0.984	-0.260	-1.600	-1.334	-3.914	-2.373	$\Delta\%$
opshrink	0.289	-1.668	-1.899	-1.785	-1.346	-4.102	-4.443	-4.235	-4.168	-4.979	$\Delta\%$
opledoitwolf	0.986	1.035	0.869	-0.010	0.984	-0.261	-1.598	-1.331	-3.906	-2.371	$\Delta\%$
opglasso	0.986	1.032	0.867	-0.010	0.984	-0.266	-1.607	-1.341	-3.920	-2.379	$\Delta\%$
MAE Min	cumulative	oplambda	opwls	opwls	oplambda	opshrink	opshrink	opshrink	opshrink	opshrink	

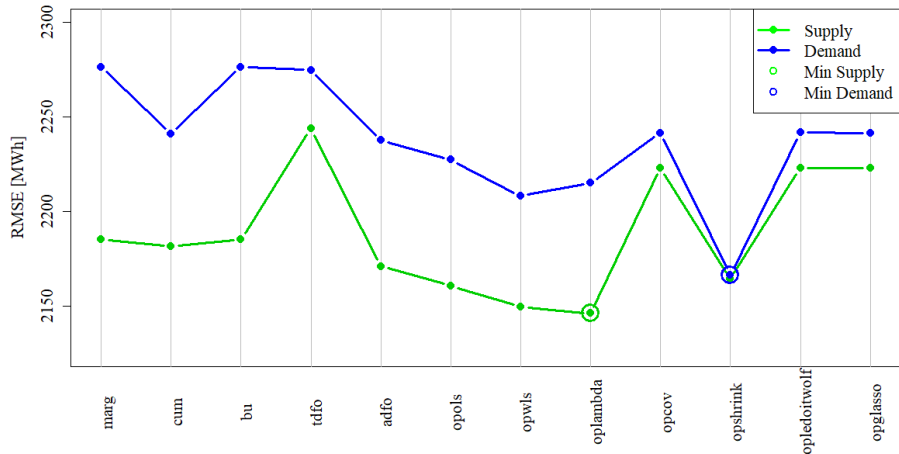
Table 5: Absolute MAE and percentage differences relative to the base case (marginal) for selected classes and reconciliation methods. Here, the marginal case is the original implementation in the X-Model paper, which corresponds to the bottom-up (bu) case.

for Figure 6. When using historical values to calculate the proportions, the top-down approach was superior to aggregated-down. However, using forecasted values to calculate the proportions for the aggregated-down approach yielded better results than the bottom-up case on average. The top-down approach still yielded less accurate values than the bottom-up approach even when using forecasted values to calculate the proportions. Hence, aggregated-down was superior to bottom-up and top-down only when using forecasted values for the proportions.

Tables 12 and 13 in the Appendix show the detailed MAEs and RMSEs over each price class. For the supply curve, no approach consistently yielded the lowest errors across all price classes. For example, the first three price classes had the lowest MAEs and RMSEs using the simple bottom-up approach. The cumulative and marginal models in the tables refer to simply forecasting all bottom-level values with the corresponding marginal or cumulative regressors and simply cumulatively summing them up, which corresponds to a bottom-up approach. It should be noted that in the results tables, the explicit bottom-up approach is equal to the cumulative approach per definition. The optimal weighted least squares (WLS) reconciliation approach yielded the lowest errors for the largest number of classes, followed by the shrinkage and lambda approaches. For the demand curve, the results were consistent for all classes, where the lowest errors were achieved by the optimal



(a) MAE



(b) RMSE

Figure 6: Average MAE and RMSE over all considered reconciliation approaches for the Supply and Demand curves.

shrinkage reconciliation approach (option 5 among the Section 3.3).

6 Conclusions

In this study, we considered the hierarchical structure of aggregated curves and different representations. We presented several reconciliation methods comprising established bottom-up, top-down, and minimum-trace optimal reconciliation approaches in an aggregated curves setting [Wickramasuriya et al., 2019]. In addition, we introduced a new

aggregated-down approach with comparable methodological complexity to the bottom-up and top-down approaches. We provided a theoretical insight that under mild assumptions regarding the forecasting and reconciling method, the reconciling result is independent of the representation of the curve. These approaches were then applied in a simulation study, and for forecasting the supply and demand curves of the German day-ahead electricity market. In the latter case, we showed that the reconciling approaches for aggregated curves can improve forecasting accuracy compared with the standard approaches.

The results showed that there is a single reconciliation method did not outperform the others every time. However, the Section 3.3 (optimal approaches), particularly the shrinkage, WLS, and lambda approaches, obtained the best results in most cases, where they obtained considerable improvements compared with the bottom-up base case. The reconciliation method that improves the forecast by the greatest amount will probably be specific to the data.

We suggest that it may be useful to consider multiple methods because even simple approaches such as Section 3.2 (aggregated-down) yielded improvements at certain points on the curve compared with the bottom-up approach, which is the current state-of-the-art method [Ziel and Steinert, 2016, 2018, Haben et al., 2021b]. Based on our finding that the top-down approach did not improve the forecasts on average whereas the aggregated-down approach using forecasted values to calculate proportions obtained improvements, we conclude that the aggregated-down approach can be applied as a simple benchmark method that is superior to top-down. In addition, we conclude that it is important to have access to all base forecasts to calculate the proportions because they can lead to substantial improvements in the forecasts compared with only using historical values.

Our study could be extended further by including more recent approaches, such as machine-learning-based [Spiliotis et al., 2021] and conditional coherency reconciliation methods [Di Fonzo and Girolimetto, 2021]. Averaging or using different reconciliation approaches for each point on the aggregated curve could also be considered, especially if coherency is not necessary.

7 Appendix

7.1 Proof of Theorem 1

Consider $\tilde{\mathbf{y}} = \mathbf{S}\mathbf{P}\hat{\mathbf{y}}$. With the definition of \mathbf{P} , $\mathbf{S} = \mathbf{B}_{[k]}\mathbf{S}_{[k]}\mathbf{A}_{[k]}\mathbf{D}_n^{-1}$, and the assumptions that $\hat{\mathbf{y}} = \mathbf{B}_{[k]}\hat{\mathbf{y}}_{[k]}$ and $\mathbf{W}_{[k]}^{-1} = \mathbf{B}'_{[k]}\mathbf{W}^{-1}\mathbf{B}_{[k]}$, it holds that:

$$\begin{aligned}
 \tilde{\mathbf{y}} &= \mathbf{S}(\mathbf{S}'\mathbf{W}^{-1}\mathbf{S})^{-1}\mathbf{S}'\mathbf{W}^{-1}\hat{\mathbf{y}} \\
 &= \mathbf{B}_{[k]}\mathbf{S}_{[k]}\mathbf{A}_{[k]}\mathbf{D}_n^{-1} \left((\mathbf{B}_{[k]}\mathbf{S}_{[k]}\mathbf{A}_{[k]}\mathbf{D}_n^{-1})' \mathbf{W}^{-1} \mathbf{B}_{[k]}\mathbf{S}_{[k]}\mathbf{A}_{[k]}\mathbf{D}_n^{-1} \right)^{-1} (\mathbf{B}_{[k]}\mathbf{S}_{[k]}\mathbf{A}_{[k]}\mathbf{D}_n^{-1})' \mathbf{W}^{-1} \hat{\mathbf{y}} \\
 &= \mathbf{B}_{[k]}\mathbf{S}_{[k]}\mathbf{A}_{[k]}\mathbf{D}_n^{-1} \left(\mathbf{D}_n \mathbf{A}_{[k]}^{-1} (\mathbf{S}'_{[k]}\mathbf{B}'_{[k]}\mathbf{W}^{-1}\mathbf{B}_{[k]}\mathbf{S}_{[k]})^{-1} (\mathbf{A}_{[k]}^{-1})' \mathbf{D}_n' \right) (\mathbf{D}_n^{-1})' \mathbf{A}'_{[k]}\mathbf{S}'_{[k]}\mathbf{B}'_{[k]}\mathbf{W}^{-1} \hat{\mathbf{y}} \\
 &= \mathbf{B}_{[k]}\mathbf{S}_{[k]} (\mathbf{S}'_{[k]}\mathbf{B}'_{[k]}\mathbf{W}^{-1}\mathbf{B}_{[k]}\mathbf{S}_{[k]})^{-1} \mathbf{S}'_{[k]}\mathbf{B}'_{[k]}\mathbf{W}^{-1}\mathbf{B}_{[k]}\hat{\mathbf{y}}_{[k]} \\
 &= \mathbf{B}_{[k]}\mathbf{S}_{[k]} (\mathbf{S}'_{[k]}\mathbf{W}_{[k]}^{-1}\mathbf{S}_{[k]})^{-1} \mathbf{S}'_{[k]}\mathbf{W}_{[k]}^{-1}\hat{\mathbf{y}}_{[k]} = \mathbf{B}_{[k]}\tilde{\mathbf{y}}_{[k]}.
 \end{aligned}$$

7.2 Results tables

No. of bottom-level values (n)	4			16			64		
No. of observations (N)	16	64	256	16	64	256	16	64	256
base	5.14	4.98	4.52	6.46	6.22	5.95	11.83	11.80	11.52
bu	5.41	5.13	4.58	7.69	7.48	7.17	18.47	21.18	20.43
tdfo	4.98	4.97	4.55	6.69	6.45	6.20	14.16	14.62	14.62
adfo	5.08	4.97	4.52	6.39	6.23	5.97	11.80	11.82	11.54
opols	5.09	4.97	4.51	6.42	6.20	5.93	11.81	11.79	11.50
opwls	5.17	5.01	4.52	6.56	6.25	5.94	11.90	11.81	11.47
oplambda	5.15	5.00	4.51	6.50	6.23	5.94	11.87	11.79	11.46
opshrink	5.22	5.05	4.56	6.82	7.07	7.72	13.21	18.57	24.27

Table 6: Simulation study RMSE results for the squared simulated values of the VAR(1) setup $\Phi = \sqrt{0.7}\mathbf{I}_n$ and $A = \mathbf{I}_n$ estimated by an AR(1) model, for selected reconciliation methods.

No. of bottom-level values (n)	4			16			64		
No. of observations (N)	16	64	256	16	64	256	16	64	256
base	5.14	4.98	4.52	6.46	6.22	5.95	11.83	11.80	11.52
bu	5.41	5.13	4.58	7.69	7.48	7.17	18.47	21.18	20.43
tdfo	4.98	4.97	4.55	6.69	6.45	6.20	14.16	14.62	14.62
adfo	5.08	4.97	4.52	6.39	6.23	5.97	11.80	11.82	11.54
opols	5.09	4.97	4.51	6.42	6.20	5.93	11.81	11.79	11.50
opwls	5.17	5.01	4.52	6.56	6.25	5.94	11.90	11.81	11.47
oplambda	5.15	5.00	4.51	6.50	6.23	5.94	11.87	11.79	11.46
opshrink	5.22	5.05	4.56	6.82	7.07	7.72	13.21	18.57	24.27

Table 7: Simulation study RMSE results for the VAR(1) setup $\Phi = 0.7I_n$ and $A = I_n$ for selected reconciliation methods, with outliers removed. Outliers were defined as simulations for which $\hat{p}_{f_{o,1}} > 50$.

No. of bottom-level values (n)	4			16			64		
No. of observations (N)	16	64	256	16	64	256	16	64	256
base	1.41	1.39	1.32	2.24	2.27	2.24	4.32	4.12	4.15
bu	1.41	1.39	1.32	2.25	2.26	2.24	4.31	4.12	4.15
tdfo	7.99	2.08	2.16	1700	16.26	13.03	163000	9040	15000
adfo	1.42	1.39	1.32	2.26	2.27	2.24	4.33	4.13	4.15
opols	1.40	1.39	1.32	2.23	2.27	2.24	4.31	4.12	4.15
opwls	1.39	1.39	1.32	2.22	2.26	2.24	4.29	4.12	4.15
oplambda	1.39	1.39	1.32	2.21	2.26	2.24	4.28	4.12	4.15
opshrink	1.40	1.39	1.32	2.23	2.27	2.24	4.34	4.13	4.15

Table 8: Simulation study RMSE results for the VAR(1) setup $\Phi = 0.5I_n$ and $A = I_n$ for selected reconciliation methods

No. of bottom-level values (n)	4			16			64		
No. of observations (N)	16	64	256	16	64	256	16	64	256
base	1.41	1.39	1.32	2.24	2.27	2.24	4.31	4.12	4.15
bu	1.40	1.39	1.32	2.24	2.26	2.24	4.31	4.13	4.15
tdfo	65.8	5.41	8.39	9670	590	889	9390000	4610	7220
adfo	1.42	1.39	1.32	2.26	2.27	2.24	4.32	4.12	4.15
opols	1.40	1.38	1.32	2.23	2.27	2.24	4.30	4.12	4.15
opwls	1.40	1.38	1.32	2.22	2.26	2.24	4.28	4.11	4.15
oplambda	1.39	1.38	1.32	2.22	2.26	2.24	4.27	4.11	4.15
opshrink	1.40	1.38	1.32	2.23	2.26	2.24	4.33	4.13	4.15

Table 9: Simulation study RMSE results for the VAR(1) setup $\Phi = 0.2I_n$ and $A = I_n$ for selected reconciliation methods

No. of bottom-level values (n)	4			16			64		
No. of observations (N)	16	64	256	16	64	256	16	64	256
base	1.41	1.39	1.32	2.26	2.26	2.24	4.35	4.14	4.15
bu	1.40	1.39	1.32	2.27	2.26	2.23	4.38	4.13	4.15
tdfo	14.9	2.71	1.55	31	20.7	574	16500	132	240
adfo	1.43	1.39	1.33	2.29	2.26	2.24	4.38	4.14	4.15
opols	1.39	1.39	1.32	2.24	2.26	2.24	4.34	4.14	4.15
opwls	1.39	1.39	1.32	2.22	2.25	2.23	4.30	4.13	4.15
oplambda	1.38	1.39	1.32	2.22	2.25	2.23	4.30	4.13	4.15
opshrink	1.39	1.39	1.32	2.24	2.26	2.23	4.35	4.14	4.15

Table 10: Simulation study RMSE results for the VAR(1) setup $\Phi = 0.95\mathbf{I}_n$ and $A = \mathbf{I}_n$ for selected reconciliation methods

No. of bottom-level values (n)	4			16			64		
No. of observations (N)	16	64	256	16	64	256	16	64	256
base	2.02	2.01	1.89	5.99	6.15	5.87	23.32	22.42	22.69
bu	2.00	2.01	1.89	5.86	6.13	5.86	22.93	22.33	22.65
tdfo	2.58	2.07	1.90	1440	6.19	5.97	30400000	23.2	23.4
adfo	2.03	2.01	1.89	6.00	6.15	5.87	23.32	22.42	22.69
opols	2.02	2.01	1.89	5.99	6.15	5.87	23.32	22.42	22.69
opwls	2.01	2.01	1.89	5.93	6.14	5.87	23.12	22.37	22.67
oplambda	2.01	2.01	1.89	5.97	6.15	5.87	23.30	22.41	22.69
opshrink	2.01	2.01	1.89	5.92	6.15	5.87	23.08	22.32	22.68

Table 11: Simulation study RMSE results for the VAR(1) setup $\Phi = 0.7\mathbf{I}_n$ and $A = 0.3\mathbf{I}_n + 0.7\mathbf{1}\mathbf{1}'$ for selected reconciliation methods

	S-500.0	S-171.5	S-99.0	S-76.0	S-49.9	S5.7	S24.0	S30.9	S35.9	S40.4	S45.0	S50.0	S57.2	S69.0	S86.5	S153.7	S260.0	S1600.0	S3000.0	Mean	
MAE	Marginal	1519	1503	1646	1827	1941	2034	2060	2010	1972	1949	1958	1956	1982	1980	1982	1981	2063	2087	1897	
	Cumulative	1535	1519	1662	1829	1941	2031	2098	1987	1956	1956	1962	1935	1974	1967	1980	1980	2050	2075	1891	
	bu	1591	1503	1646	1827	1941	2034	2060	2010	1971	1949	1957	1956	1982	1980	1982	1981	2063	2087	1897	
	tdar	3496	3191	2765	2354	2503	2680	2804	2820	2694	2532	2364	2277	2188	2064	2020	2031	2001	2047	2068	2468
	tdra	3430	3142	2733	2358	2507	2671	2808	2829	2704	2546	2381	2289	2196	2072	2027	2037	2004	2048	2068	2466
	tdfo	1781	1703	1666	1756	1889	1993	2087	2111	2045	2003	1972	1968	1954	1976	1973	1986	1975	2045	2068	1945
	adar	1591	1498	1568	2171	2832	3189	3189	3117	2969	2882	2804	2848	2886	2966	2965	2975	3017	3141	3198	2727
	adra	1591	1498	1568	2133	2769	3104	3122	3061	2910	2824	2753	2797	2842	2927	2934	2951	2997	3127	3186	2689
	adfo	1591	1495	1518	1642	1808	1921	2009	2079	1972	1942	1941	1948	1922	1962	1957	1969	1970	2041	2068	1882
	opls	1583	1506	1513	1635	1800	1909	2009	2043	1974	1941	1922	1928	1917	1951	1953	1967	1962	2037	2063	1874
	opwls	1639	1553	1534	1643	1796	1900	1997	2021	1963	1928	1900	1901	1896	1931	1934	1947	1937	2009	2033	1866
	oplambda	1587	1511	1511	1631	1794	1900	1998	2024	1965	1931	1903	1906	1901	1936	1940	1954	1944	2017	2041	1863
	opcov	1606	1566	1557	1687	1846	1958	2051	2072	2010	1978	1956	1961	1963	2002	2007	2016	2002	2067	2087	1915
	opshrink	1595	1535	1526	1644	1797	1904	1993	2017	1959	1928	1908	1910	1909	1952	1959	1972	1963	2029	2050	1871
	opledotwolf	1606	1566	1557	1687	1846	1958	2051	2072	2010	1978	1956	1961	1963	2002	2007	2016	2002	2067	2087	1915
	opglasso	1606	1566	1557	1687	1846	1958	2051	2072	2010	1978	1956	1961	1963	2002	2008	2016	2002	2067	2087	1915
MAE Minimum	Cumulative	1846	1771	1756	1911	2097	2330	2361	2316	2273	2249	2254	2251	2282	2275	2279	2283	2367	2393	2185	
Marginal	1788	1746	1771	1926	2099	2230	2329	2397	2294	2256	2264	2262	2236	2276	2268	2284	2285	2355	2379	2181	
Cumulative	1846	1771	1756	1911	2097	2228	2330	2361	2316	2273	2249	2254	2251	2282	2275	2279	2283	2367	2393	2185	
bu	3831	3522	3109	2680	2821	3021	3150	3161	3022	2855	2681	2590	2495	2363	2316	2331	2302	2350	2370	2788	
tdar	3769	3477	3081	2685	2823	3012	3150	3167	3030	2866	2696	2601	2501	2368	2324	2338	2305	2351	2370	2785	
tdra	2051	1973	1945	2043	2179	2301	2397	2420	2357	2313	2283	2274	2257	2280	2274	2287	2278	2347	2370	2244	
tdfo	1846	1749	1826	2447	3139	3519	3526	3460	3330	3244	3176	3229	3275	3370	3378	3394	3450	3589	3650	3084	
adar	1846	1749	1826	2409	3073	3433	3455	3404	3271	3187	3123	3178	3230	3331	3349	3371	3431	3574	3637	3046	
adra	1846	1746	1771	1906	2077	2209	2307	2377	2275	2239	2246	2247	2223	2264	2256	2271	2274	2344	2370	2171	
adfo	1835	1754	1763	1898	2069	2197	2302	2340	2271	2235	2224	2224	2213	2249	2249	2265	2263	2338	2364	2161	
opls	1893	1804	1786	1909	2067	2189	2289	2314	2257	2218	2194	2192	2186	2222	2225	2238	2231	2303	2326	2150	
opwls	1840	1759	1760	1893	2062	2187	2289	2317	2259	2221	2199	2199	2193	2229	2232	2247	2240	2313	2337	2146	
oplambda	1881	1834	1829	1977	2143	2275	2375	2395	2331	2293	2274	2276	2277	2318	2320	2332	2319	2384	2405	2223	
opcov	1856	1792	1787	1919	2080	2207	2303	2326	2266	2229	2213	2212	2209	2253	2258	2270	2261	2329	2351	2164	
opshrink	1881	1834	1829	1977	2143	2275	2375	2395	2331	2293	2274	2276	2277	2318	2320	2332	2319	2384	2405	2223	
opledotwolf	1881	1834	1829	1977	2143	2275	2375	2395	2331	2293	2274	2276	2277	2318	2320	2332	2319	2384	2405	2223	
opglasso	1881	1834	1829	1977	2143	2275	2375	2395	2331	2293	2274	2276	2277	2318	2320	2332	2319	2384	2405	2223	
RMSE Minimum	Cumulative	1846	1771	1756	1911	2097	2330	2361	2316	2273	2249	2254	2251	2282	2275	2279	2283	2367	2393	2185	
Marginal	1788	1746	1771	1926	2099	2230	2329	2397	2294	2256	2264	2262	2236	2276	2268	2284	2285	2355	2379	2181	
Cumulative	1846	1771	1756	1911	2097	2228	2330	2361	2316	2273	2249	2254	2251	2282	2275	2279	2283	2367	2393	2185	
bu	3831	3522	3109	2680	2821	3021	3150	3161	3022	2855	2681	2590	2495	2363	2316	2331	2302	2350	2370	2788	
tdar	3769	3477	3081	2685	2823	3012	3150	3167	3030	2866	2696	2601	2501	2368	2324	2338	2305	2351	2370	2785	
tdra	2051	1973	1945	2043	2179	2301	2397	2420	2357	2313	2283	2274	2257	2280	2274	2287	2278	2347	2370	2244	
tdfo	1846	1749	1826	2447	3139	3519	3526	3460	3330	3244	3176	3229	3275	3370	3378	3394	3450	3589	3650	3084	
adar	1846	1749	1826	2409	3073	3433	3455	3404	3271	3187	3123	3178	3230	3331	3349	3371	3431	3574	3637	3046	
adra	1846	1746	1771	1906	2077	2209	2307	2377	2275	2239	2246	2247	2223	2264	2256	2271	2274	2344	2370	2171	
adfo	1835	1754	1763	1898	2069	2197	2302	2340	2271	2235	2224	2224	2213	2249	2249	2265	2263	2338	2364	2161	
opls	1893	1804	1786	1909	2067	2189	2289	2314	2257	2218	2194	2192	2186	2222	2225	2238	2231	2303	2326	2150	
opwls	1840	1759	1760	1893	2062	2187	2289	2317	2259	2221	2199	2199	2193	2229	2232	2247	2240	2313	2337	2146	
oplambda	1881	1834	1829	1977	2143	2275	2375	2395	2331	2293	2274	2276	2277	2318	2320	2332	2319	2384	2405	2223	
opcov	1856	1792	1787	1919	2080	2207	2303	2326	2266	2229	2213	2212	2209	2253	2258	2270	2261	2329	2351	2164	
opshrink	1881	1834	1829	1977	2143	2275	2375	2395	2331	2293	2274	2276	2277	2318	2320	2332	2319	2384	2405	2223	
opledotwolf	1881	1834	1829	1977	2143	2275	2375	2395	2331	2293	2274	2276	2277	2318	2320	2332	2319	2384	2405	2223	
opglasso	1881	1834	1829	1977	2143	2275	2375	2395	2331	2293	2274	2276	2277	2318	2320	2332	2319	2384	2405	2223	
RMSE	Cumulative	1846	1771	1756	1911	2097	2330	2361	2316	2273	2249	2254	2251	2282	2275	2279	2283	2367	2393	2185	
Marginal	1788	1746	1771	1926	2099	2230	2329	2397	2294	2256	2264	2262	2236	2276	2268	2284	2285	2355	2379	2181	
Cumulative	1846	1771	1756	1911	2097	2228	2330	2361	2316	2273	2249	2254	2251	2282	2275	2279	2283	2367	2393	2185	
bu	3831	3522	3109	2680	2821	3021	3150	3161	3022	2855	2681	2590	2495	2363	2316	2331	2302	2350	2370	2788	
tdar	3769	3477	3081	2685	2823	3012	3150	3167	3030	2866	2696	2601	2501	2368	2324	2338	2305	2351	2370	2785	
tdra	2051	1973	1945	2043	2179	2301															

	D3000.0	D1001.1	D50.1	D155.1	D76.0	D50.1	D42.1	D35.5	D30.1	D25.1	D19.1	D11.1	D7.0	D-6.9	D-58.9	D-76.9	D-90.0	D-146.0	D-180.0	D-388.8	D-500.0	Mean	
MAE	Marginal	2051	2042	2005	2003	1962	1964	1946	1961	1969	1958	1952	1951	1966	2005	1906	1818	1883	1913	1942	1957	1957	
	Cumulative	1990	1998	1945	1932	1893	1883	1866	1874	1937	1950	1946	1968	1992	2039	1893	1803	1894	1961	1984	2010	1935	1935
	bu	2781	2790	2827	2801	2616	2343	2210	2116	2161	2070	1940	1911	1934	1944	1895	1816	1883	1913	1942	1957	1957	1957
	tdar	2767	2775	2812	2784	2602	2473	2340	2209	2120	2083	1945	1910	1932	1941	1892	1816	1899	1983	2021	2015	2214	2214
	tdfo	2042	2032	1976	1973	1944	1929	1945	1925	1939	1960	1961	1966	1969	1989	2040	1929	1845	1930	1967	1994	2015	1965
	adar	2051	2043	2028	1991	1932	2011	2104	2104	2244	2344	2321	2517	2829	2983	2940	2053	2779	2806	2911	3013	3042	2467
	adra	2051	2044	2032	1995	1934	1963	2001	2085	2215	2309	2280	2460	2765	2922	2873	2879	2713	2744	2847	2942	2968	2430
	adfo	2051	1996	1944	1928	1889	1863	1869	1851	1854	1915	1926	1930	1958	1983	2030	1886	1804	1899	1967	1987	2015	1931
	opols	2023	1996	1940	1925	1879	1854	1862	1845	1862	1901	1911	1923	1943	1965	2018	1890	1803	1898	1951	1985	2009	1923
	opwks	1992	1984	1932	1917	1874	1855	1868	1851	1867	1894	1893	1897	1902	1919	1979	1869	1781	1887	1927	1956	1978	1906
	oplambda	2026	1999	1942	1926	1878	1855	1865	1847	1863	1891	1892	1900	1910	1930	1991	1880	1794	1886	1929	1960	1983	1912
	opcov	2045	2031	1975	1932	1900	1883	1890	1874	1895	1925	1919	1918	1919	1940	1994	1866	1788	1835	1851	1869	1881	1911
	opshrink	1967	1957	1904	1879	1844	1823	1831	1818	1833	1863	1860	1860	1864	1883	1940	1823	1739	1803	1834	1860	1876	1860
	opledotwolf	2045	2031	1975	1932	1900	1883	1890	1874	1895	1925	1919	1919	1920	1940	1994	1866	1788	1835	1851	1869	1881	1911
	opgasso	2045	2031	1975	1932	1900	1883	1890	1874	1894	1924	1918	1918	1919	1940	1993	1866	1788	1835	1851	1869	1881	1911
RMSE	MAE Minimum	opshrink	opshrink	opshrink	opshrink	opshrink	opshrink	opshrink	opshrink	opshrink	opshrink	opshrink	opshrink	opshrink	opshrink	opshrink	opshrink	opshrink	opshrink	opshrink	opshrink	opshrink	
	Marginal	2377	2367	2337	2329	2284	2273	2284	2267	2276	2284	2276	2273	2272	2291	2328	2224	2133	2194	2221	2247	2263	2276
	Cumulative	2324	2320	2269	2257	2210	2190	2200	2174	2179	2241	2249	2244	2268	2298	2343	2188	2100	2183	2251	2272	2301	2241
	bu	2377	2367	2337	2329	2284	2273	2284	2267	2276	2284	2276	2273	2272	2291	2328	2224	2133	2194	2221	2247	2263	2276
	tdar	3129	3140	3173	3142	2948	2802	2673	2541	2443	2488	2393	2263	2234	2259	2262	2207	2120	2195	2278	2310	2305	2538
	tdra	3117	3127	3161	3127	2935	2795	2671	2540	2447	2498	2406	2269	2233	2258	2260	2205	2120	2197	2279	2311	2305	2536
	tdfo	2359	2350	2299	2291	2258	2246	2264	2244	2253	2276	2274	2277	2281	2302	2348	2230	2147	2223	2259	2284	2305	2275
	adar	2377	2370	2356	2311	2250	2298	2350	2448	2586	2685	2660	2847	3149	3305	3264	3270	3099	3109	3215	3322	3351	2791
	adra	2377	2371	2359	2315	2251	2294	2340	2429	2558	2650	2620	2791	3088	3247	3199	3199	3033	3049	3154	3253	3278	2755
	adfo	2377	2317	2269	2254	2207	2186	2189	2160	2160	2220	2227	2230	2258	2289	2333	2182	2104	2188	2257	2275	2305	2237
	opols	2344	2313	2263	2246	2195	2173	2178	2155	2166	2203	2209	2222	2241	2269	2319	2183	2098	2186	2240	2272	2298	2227
	opwks	2307	2297	2252	2235	2186	2167	2178	2160	2172	2196	2192	2196	2201	2224	2280	2161	2075	2174	2213	2241	2262	2208
	oplambda	2347	2316	2264	2245	2192	2171	2177	2157	2168	2193	2191	2199	2209	2235	2291	2172	2087	2174	2215	2245	2267	2215
	opcov	2401	2385	2329	2277	2235	2217	2223	2208	2226	2255	2245	2243	2243	2268	2319	2186	2103	2153	2170	2187	2200	2242
	opshrink	2286	2274	2224	2197	2155	2136	2144	2130	2144	2171	2166	2167	2169	2192	2245	2121	2039	2098	2125	2148	2164	2166
opledotwolf	2401	2385	2329	2277	2235	2217	2223	2208	2227	2255	2245	2243	2243	2268	2319	2186	2103	2153	2170	2187	2200	2242	
opgasso	2401	2385	2329	2276	2235	2217	2223	2208	2226	2254	2245	2243	2242	2268	2319	2186	2103	2153	2170	2187	2199	2241	
RMSE Minimum	opshrink	opshrink	opshrink	opshrink	opshrink	opshrink	opshrink	opshrink	opshrink	opshrink	opshrink	opshrink	opshrink	opshrink	opshrink	opshrink	opshrink	opshrink	opshrink	opshrink	opshrink	opshrink	

Table 13: MAE and RMSE for the Demand curve and all considered reconciliation methods

References

- A. Marshall. Principles of economics: unabridged eighth edition. Cosimo, Inc., 2009.
- N. G. Mankiw. Principles of economics. Cengage Learning, 2014.
- R. S. Pindyck, D. L. Rubinfeld, and P. L. Mehta. Microeconomics, volume 4. Prentice Hall Englewood Cliffs, NJ, 1995.
- J. C. Hull. Options futures and other derivatives. Pearson Education India, 2003.
- R. S. Gürkaynak, B. Sack, and J. H. Wright. The us treasury yield curve: 1961 to the present. Journal of monetary Economics, 54(8):2291–2304, 2007.
- J. Aitchison and J. A. Brown. A synthesis of engel curve theory. The Review of Economic Studies, 22(1):35–46, 1954.
- J. Banks, R. Blundell, and A. Lewbel. Quadratic engel curves and consumer demand. Review of Economics and statistics, 79(4):527–539, 1997.
- A. W. Phillips. The relation between unemployment and the rate of change of money wage rates in the united kingdom, 1861-1957. Economica, 25(100):283–299, 1958. ISSN 00130427, 14680335. URL <http://www.jstor.org/stable/2550759>.
- W. J. Eiteman and G. E. Guthrie. The shape of the average cost curve. The American economic review, 42(5):832–838, 1952.
- F. Ziel and R. Steinert. Electricity price forecasting using sale and purchase curves: The x-model. Energy Economics, 59:435–454, 2016. ISSN 0140-9883. doi: <https://doi.org/10.1016/j.eneco.2016.08.008>. URL <https://www.sciencedirect.com/science/article/pii/S0140988316302080>.
- H. L. Shang and R. J. Hyndman. Grouped functional time series forecasting: An application to age-specific mortality rates. Journal of Computational and Graphical Statistics, 26(2):330–343, 2017.
- R. J. Hyndman and M. S. Ullah. Robust forecasting of mortality and fertility rates: A functional data approach. Computational Statistics & Data Analysis, 51(10):4942–4956, 2007.

- H. L. Shang and R. J. Hyndman. Nonparametric time series forecasting with dynamic updating. Mathematics and Computers in Simulation, 81(7):1310–1324, 2011.
- R. J. Hyndman and G. Athanasopoulos. Forecasting: principles and practice. OTexts, 2018. URL <https://otexts.com/fpp2/>.
- S. L. Wickramasuriya, G. Athanasopoulos, and R. J. Hyndman. Optimal forecast reconciliation for hierarchical and grouped time series through trace minimization. Journal of the American Statistical Association, 114(526):804–819, 2019. URL <https://www.tandfonline.com/doi/full/10.1080/01621459.2018.1448825>.
- E. Spiliotis, M. Abolghasemi, R. J. Hyndman, F. Petropoulos, and V. Assimakopoulos. Hierarchical forecast reconciliation with machine learning. Applied Soft Computing, page 107756, 2021.
- T. Van Erven and J. Cugliari. Game-theoretically optimal reconciliation of contemporaneous hierarchical time series forecasts. In Modeling and stochastic learning for forecasting in high dimensions, pages 297–317. Springer, 2015.
- T. Di Fonzo and D. Girolimetto. Forecast combination based forecast reconciliation: insights and extensions. arXiv preprint arXiv:2106.05653, 2021.
- R. Hollyman, F. Petropoulos, and M. E. Tipping. Understanding forecast reconciliation. European Journal of Operational Research, 294(1):149–160, 2021.
- M. Brégère and M. Huard. Online hierarchical forecasting for power consumption data. International Journal of Forecasting, 38(1):339–351, 2022.
- M. Huard, R. Garnier, and G. Stoltz. Hierarchical robust aggregation of sales forecasts at aggregated levels in e-commerce, based on exponential smoothing and holt’s linear trend method. arXiv preprint arXiv:2006.03373, 2020.
- M. Narajewski and F. Ziel. Optimal bidding in hourly and quarter-hourly electricity price auctions: trading large volumes of power with market impact and transaction costs. Energy Economics, 110:105974, 2022.
- F. Ziel and R. Steinert. Probabilistic mid-and long-term electricity price forecasting. Renewable and Sustainable Energy Reviews, 94:251–266, 2018.

- S. Haben, J. Caudron, and J. Verma. Probabilistic day-ahead wholesale price forecast: A case study in great britain. Forecasting, 3(3):596–632, 2021a.
- S. Kulakov. X-model: Further development and possible modifications. Forecasting, 2(1): 20–35, 2020.
- G. Mestre, J. Portela, A. M. San Roque, and E. Alonso. Forecasting hourly supply curves in the italian day-ahead electricity market with a double-seasonal sarmahx model. International Journal of Electrical Power & Energy Systems, 121:106083, 2020.
- M. Soloviova and T. Vargiolu. Efficient representation of supply and demand curves on day-ahead electricity markets. Journal of Energy Markets, 14(1), 2021.
- C. W. Gross and J. E. Sohl. Disaggregation methods to expedite product line forecasting. Journal of forecasting, 9(3):233–254, 1990.
- J. Schäfer and K. Strimmer. A shrinkage approach to large-scale covariance matrix estimation and implications for functional genomics. Statistical applications in genetics and molecular biology, 4(1), 2005.
- O. Ledoit and M. Wolf. Honey, i shrunk the sample covariance matrix. The Journal of Portfolio Management, 30(4):110–119, 2004.
- J. Friedman, T. Hastie, and R. Tibshirani. Sparse inverse covariance estimation with the graphical lasso. Biostatistics, 9(3):432–441, 2008.
- F. Petropoulos, D. Apiletti, V. Assimakopoulos, M. Z. Babai, D. K. Barrow, S. B. Taieb, et al. Forecasting: theory and practice. International Journal of Forecasting, 2022.
- M. Soloviova. Modeling of supply and demand curves for day-ahead electricity market. Seminario Dottorato 2019/20, page 113.
- S. Haben, J. Caudron, and J. Verma. Probabilistic day-ahead wholesale price forecast: A case study in great britain. Forecasting, 3(3):596–632, 2021b. ISSN 2571-9394. doi: 10.3390/forecast3030038. URL <https://www.mdpi.com/2571-9394/3/3/38>.